AAS 19-345

HYBRID CHEMICAL-ELECTRIC TRAJECTORIES FOR A MARS SAMPLE RETURN ORBITER

Frank Laipert[*], Austin Nicholas[†], Zubin Olikara[†], Ryan Woolley[†], and Rob Lock[†]

The Earth return orbiter component of a Mars sample return campaign is a high total impulse mission with challenging timeline constraints. These competing demands mean a hybrid chemical-electric propulsion architecture may be needed for a feasible design, with chemical propulsion providing timely impulse and electric propulsion providing high volume impulse. We describe an approach to map out the hybrid trajectory design space and create a database to use in conjunction with a spacecraft design tool, enabling co-optimization of trajectory and spacecraft. This method is applied to both the outbound and inbound legs of a Mars sample return mission concept.

INTRODUCTION

Acquiring a geological sample from the surface of Mars has long been a major goal for the planetary science community, and in the most recent decadal survey was singled out as the highest priority flagship mission for NASA to conduct[1]. Mission design and architecture work on a Mars sample return campaign stretches back decades, but most recently a "lean" architecture that focuses only sample return (without other scientific objectives) has been of primary interest. This potential architecture would be a partnership between NASA and ESA, with NASA responsible for the Sample Return Lander (SRL) and ESA responsible for the Earth Return Orbiter (ERO). The ERO is tasked with capturing the orbiting sample container (OS) after it has been injected into low-Mars orbit by the Mars Ascent Vehicle (MAV) and returning it safely back to the surface of Earth for scientists to study. In addition, recent technological developments in solar electric propulsion (SEP) has added a new capability that may not have been seriously considered in previous studies. In this study, we present a method for searching for trajectories that employ both chemical and solar electric propulsion technologies and apply it to the ERO element of a multifaceted Mars sample return campaign.

Returning from Mars to Earth is a major challenge not faced by any previous Mars orbiter. The Δv required to complete this mission is much higher than a one-way mission, and it is especially difficult to perform with an all-chemical mission. In contrast, the much higher efficiency of solar electric propulsion allows it to handle the higher Δv needs, but in general such a spacecraft requires longer transfer times between Earth and Mars compared to a chemical spacecraft. For a Mars sample return mission, time is a particularly important constraint because of the interactions between the orbital and surface missions, especially the timing of the MAV launch. The surface mission is further constrained by its own launch and arrival window and the seasons on Mars. Therefore, combining both chemical and solar electric propulsion technologies on the orbiter may be necessary for the mission to succeed. Hybrid chemical-electric propulsion has previously been considered for round-trip Mars missions in the context of human exploration. Strange et al. found mass savings of up to 60% using hybrid propulsion[2]. While a sample return mission is much smaller in scale, the Δv requirements are similar to a human mission.

[*]Corresponding Author; *Mailing Address*: Jet Propulsion Laboratory, California Institute of Technology, 4800 Oak Grove Drive, Pasadena, CA, 91109; *Tel*: (818) 393-8051; *Email*: Frank.E.Laipert@jpl.caltech.edu
[†]Jet Propulsion Laboratory, California Institute of Technology, Pasadena, CA, 91109

APPROACH

For any mission using electric propulsion, the trajectory design is tightly coupled with the spacecraft bus design. This coupling is a significant complication over a purely chemical mission, where the trajectory can largely be designed independent of the spacecraft. This means that for this study, we cannot design an "optimal" trajectory using chemical and SEP technology, and then separately design a spacecraft to fly it. At the same time, creating an all-encompassing optimization tool in the traditional sense that includes both the trajectory and all the important aspects of the spacecraft bus is impractical. Instead, our approach, and the focus of this paper, is to extensively map out the trajectory design space and create a database of pre-computed trajectories which span the possible propulsion and power technologies available for the spacecraft. This database can then serve as the trajectory component of a spacecraft systems optimization tool that iteratively designs the bus and matches it to a trajectory while improving some desired parameter. The particular tool the database is intended for is the Mars Orbiter Tool (MORT) described by Nicholas in [3]. Using a trajectory database approach, as opposed to building the optimizer directly into the system design tool, also carries a computation speed benefit which has been found to be as much as a sixfold reduction in processing time.

Mission Phases

The complicated nature of a Mars sample return mission means breaking it up into separate phases is necessary for the trajectory design problem. We identify the following primary phases in the sample return orbiter mission concept:

1. **Launch**. The mission begins with launch from Earth. We model the launch vehicle performance as polynomial function of the launch C_3 and include it in the optimization of the next phase.
2. **Outbound Transfer**. After launch, the orbiter travels from Earth to Mars using its SEP system. In contrast to a pure SEP mission, it may arrive at Mars with some positive v_∞.
3. **Mars Orbit Insertion**. Upon arrival at Mars, a large orbit insertion maneuver is performed using the chemical propulsion system.
4. **Spiral Down**. After MOI, the orbiter uses its SEP system to spiral from the highly elliptical capture orbit down to low Mars orbit (LMO). We do not consider the use of aerobraking in this phase, as it was found to be of little to no help compared with the SEP spiral.
5. **Low Mars Orbit**. In LMO, the orbiter provides support to the surface mission, observes the sample launch, and captures the orbiting sample (OS). Of primary relevance to the trajectory design, a staging event occurs allowing the spacecraft to drop hardware mass that is no longer needed before returning to Earth.
6. **Spiral Up**. The orbiter uses its SEP system to begin raising its orbit to depart Mars. It may use either a circular spiral for a pure SEP departure, or an elliptical spiral if a chemical burn will occur.
7. **Trans-Earth Injection**. A chemical burn may be performed to depart Mars with a positive v_∞.
8. **Inbound Transfer**. The orbiter returns to Earth using its SEP system. It will arrive with a positive v_∞.
9. **Earth Arrival**. Upon arrival at Earth, the orbiter separates from the Earth Entry Vehicle (EEV) containing the samples. The EEV enters the atmosphere while the orbiter performs a divert maneuver to avoid entry.

Constraints

For the purposes of this study, we consider ERO launch dates as early as 2026 and as late as 2029, with a focus on 2026 as the primary launch year. The samples can be returned to Earth as early as 2029 and as late as 2034. We assume the Ariane 6.4 launch vehicle, which is currently in development. To comply with the Ariane launch site in Kourou, French Guinana, the launch declination is constrained to be between -5° and +5°. A launch vehicle adapter mass of 110 kg and a launch mass contigency of 10% is used.

Trajectory Database

The primary product of the mission analysis is a trajectory database that can be queried by a spacecraft system design tool to produce an optimal, matched spacecraft-trajectory pair that meets the mission constraints. For the outbound, Earth-to-Mars transfers, the database should yield a trajectory for any pair of launch date and LMO arrival date that has the maximum mass delivered to LMO. For the inbound, Mars-to-Earth transfers, the database should yield a trajectory for any pair of LMO departure date and Earth arrival date that delivers a specified mass to Earth with a minimum mass at LMO departure. To do this, we iterate over a wide range of variables and exhaustively map out the trajectory design space. By taking this approach, we can have increased confidence that a given solution is close to globally optimal.

Outbound Database To create the outbound database, we perform a multi-dimensional grid search over the following variables: 1) propulsion system, 2) power level, 3) launch date, 4) heliocentric time-of-flight, 5) Mars arrival v_∞, and 6) LMO arrival date. Each of these variables is discretized into a finite grid. Table 1 contains a more detailed listing of the outbound search grid.

Table 1: The grid search definition for the outbound transfers.

Variable	Lower Bound	Upper Bound	Step Size	Total Grid Points
Propulsion Configurations	-	-	-	30
Power at 1 AU	11 kW	120 kW	-	9–11[a]
Launch Date	5-Mar-2025	12-Jun-2029	20 d	79
Heliocentric TOF	100 d	1600 d	20 d	76
Mars Arrival v_∞	0.0 km/s	3.0 km/s	0.2 km/s	16
Total	-	-	-	29,683,776

[a] The power levels in the grid are different for each propulsion configuration.

For every grid point of variables 1–5, we design an optimal low-thrust trajectory using the MALTO medium-fidelity design tool [4]. Given a fixed propulsion system, power level, launch date, time-of-flight, and Mars arrival v_∞, MALTO finds an optimal trajectory solution that fits within the performance envelope of the launch vehicle. Then, for every grid point for LMO arrival date, an optimal transfer from hyperbolic Mars arrival to LMO is designed for all available combinations of launch date, heliocentric TOF, and arrival v_∞, resulting in many possible trajectories that reach LMO on the desired date. Each transfer begins with an MOI to capture into an elliptical orbit, and then the SEP system is used to spiral down to LMO. The spiral to LMO is a minimum-propellant spiral computed using an averaging method developed by Olikara [5]. From these trajectories, the one that delivers the most mass to LMO is selected. This selection effectively eliminates arrival v_∞ as one dimension from the database. The resulting database is also converted from having regular spacing heliocentric TOF to having regular spacing in total launch-to-LMO time of flight.

The optimization of the spiral to LMO is illustrated with an example in Figure 1. In this example, only one pair of Earth launch date and LMO arrival date is represented, with launch on June 28, 2026 and LMO arrival on February 18, 2028. Because the dates are fixed, the total TOF is set to 600 days, which must be split between the heliocentric transfer and the spiral down to LMO. In the plot, we can see that for very low heliocentric TOF, only a low initial mass is available because the spacecraft must launch to a high C3 to reach Mars quickly. As the heliocentric TOF is extended, more initial mass is available due to a more favorable heliocentric trajectory. In the intermediate range of heliocentric TOF, the Δv is still primarily accomplished by the EP system, with the CP system providing only the MOI to a high apoapsis and more time spent spiraling. At much higher TOF solutions, little time is available to spiral, resulting in a larger MOI into a lower capture orbit, using more chemical propellant. These high TOF solutions are skewed more towards the chemical side of the chemical-SEP hybrid architecture. In terms of mass delivered to LMO, an optimum exists with a 480 day heliocentric transfer and 120 day spiral.

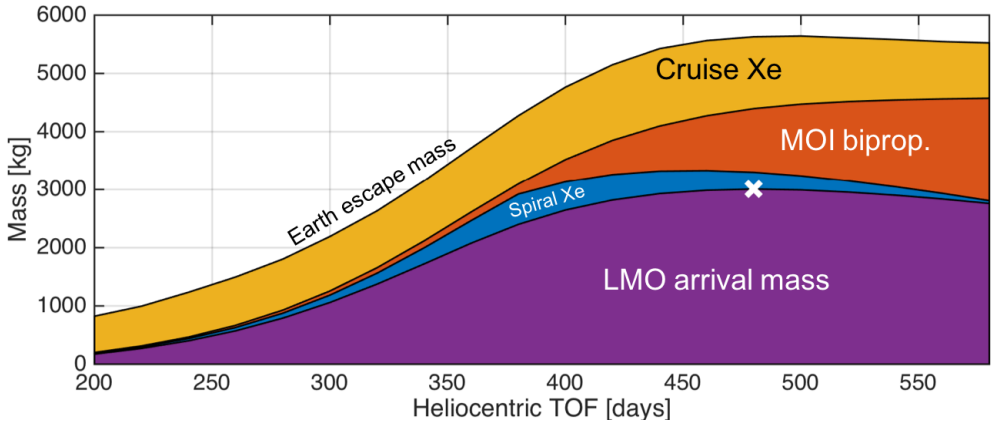

Figure 1: The trade between heliocentric TOF and spiral TOF is shown for a single pair of Earth launch and LMO arrival dates. All solutions launch from Earth on the same date and arrive at LMO on the same date, and the optimum arrival v_∞ is chosen for each heliocentric TOF.

Inbound Database The inbound database is built in a similar manner to the outbound database, however some of the grid variables are different. First, because of the advantage of dropping the chemical propulsion stage at Mars, it was decided that the inbound transfers would be strictly SEP-based. Therefore, no TEI is considered, and the Mars departure v_∞ is fixed at 0 km/s. Second, an additional dimension of Earth arrival mass is included in the inbound grid. For each arrival mass, the heliocentric trajectory is optimized to minimize Mars departure mass. Third, three values for Earth arrival v_∞ are considered. Details of the inbound grid search variables are shown in Table 2.

Table 2: The grid search definition for the inbound transfers.

Variable	Lower Bound	Upper Bound	Step Size	Total Grid Points
Propulsion Configurations	-	-	-	30
Power at 1 AU	11 kW	120 kW	-	9–11[a]
Departure Date	24-Apr-2027	19-Sep-2033	20 d	118
Heliocentric TOF	100 d	1600 d	20 d	76
Mars Departure v_∞	0.0 km/s	0.0 km/s	0.0 km/s	1
Earth Arrival v_∞ Constraint	1.5 km/s	6.8 km/s	-	3[b]
Earth Arrival Mass	750	3500	-	5–10[c]
Total	-	-	-	68,901,144

[a] The power levels in the grid are different for each propulsion configuration.
[b] Arrival v_∞ constraint is not a regular grid. Values are 1.5, 4.5 and 6.8 km/s, which are chosen to represent various EDL capabilities.
[c] The arrival mass levels in the grid are different for each propulsion configuration.

SEP Thrusters We considered the RIT 2X, T6, PPS, and Hermes thrusters for the the SEP propulsion system. The RIT and T6 are gridded ion engines, while the PPS and Hermes are Hall effect thrusters. For the RIT, T6, and PPS, we examined the use of between 2 and 8 thrusters, and for the Hermes we considered one or two thrusters. In addition, the PPS was analyzed in two different operating modes: high thrust and high specific impulse. Each thruster was modeled using polynomial curve fits of the thrust and propellant mass flow rate vs input power. Table 3 contains performance data for the thrusters included in this study. Because the ERO would be developed by ESA, focus was placed on European thruster technologies, with the RIT, T6,

and PPS being produced by European companies.

Table 3: SEP Thruster Characteristics

Thruster	Max Power, kW	Max Thrust, mN	Specific Impulse, sec	Efficiency, %
RIT 2X	6.3	190	3880	57
T6	5.0	145	3900	55
PPS	5.5	292	1750	46
Hermes	13.5	611	2800	62

Computing This exhaustive trajectory database is useful for the spacecraft design, since a program that is sizing the spacecraft and its main subsystems can simply choose a trajectory that meets the mass and timeline constraints. However, creating the database is computationally challenging. Between the outbound and inbound legs, over 98 million separate trajectory optimizations are needed to reach every point in the grids defined in Tables 1 and 2.

Fortunately, each of these optimizations is independent and may be done in parallel. We use the Nexus computing cluster at JPL to create the database. Nexus has 32 nodes, and each node has 16 computing cores, for a maximum total of 512 parallel processes. However, because it is a shared resource, we limited our use to around one third to one half of the processes at any given time. With these computing resources, we are able to generate trajectories at an average of 100 *traps*, where one traps is one trajectory per second. At this rate, it takes 11.3 days to build the database, running non-stop. Building the database with only one process, we estimate that it would take over 6 years to create.

RESULTS

Outbound Results

The results of the grid search are best visualized as a bacon plot, which is a low thrust version of the pork chop plot [6]. An example of a bacon plot is shown in Figure 2. The plot applies for only one thruster configuration and power level—three RIT 2X thrusters at 28 kW. On the horizontal axis is launch date from Earth, and on the vertical axis is arrival date at LMO. For each launch-arrival date pair, the optimum balance of heliocentric TOF, spiral TOF, and arrival v_∞ has been chosen, considering the propellant mass used in the heliocentric transfer, MOI, and the spiral to LMO. We can see that, for a given LMO mass, there is an ideal launch date that allows for the earliest arrival date at LMO. In the case shown here, a launch in September 2026 delivers the most mass to LMO at an earlier arrival date.

The case shown in Figure 2 is only a small portion of all the data generated in the grid search. The equivalent data for thousands of other configurations was generated, meaning that it is impractical to plot each case and have a human examine it. Instead, the data is kept in a machine readable form, so that another software tool may query it for trajectory solutions.

The black dot in Figure 2 marks a pair of launch and arrival dates for a point design selected as a baseline for further study. The point design was selected as part of the system optimization, considering the trajectory as well as factors not covered in this paper, such as power system mass and propellant tank mass [7]. We can see that the solution is located in a region of higher delivered masses at later launch dates. It has a launch date of September 27, 2026 and an arrival date in LMO of October 25, 2028, delivering 4165 kg of total mass. Examining the region around the solution, we can see it would be possible to deliver more mass by delaying arrival in LMO and maintaining the same launch date. However, this would impact the surface mission and is not desirable for that reason. In addition, delaying the launch date quickly results in a steep decrease in performance.

Interestingly, there are two families of solutions present which deliver similar mass to LMO around the same date. One family, which the baseline solution is located in, has later launch dates, while the other

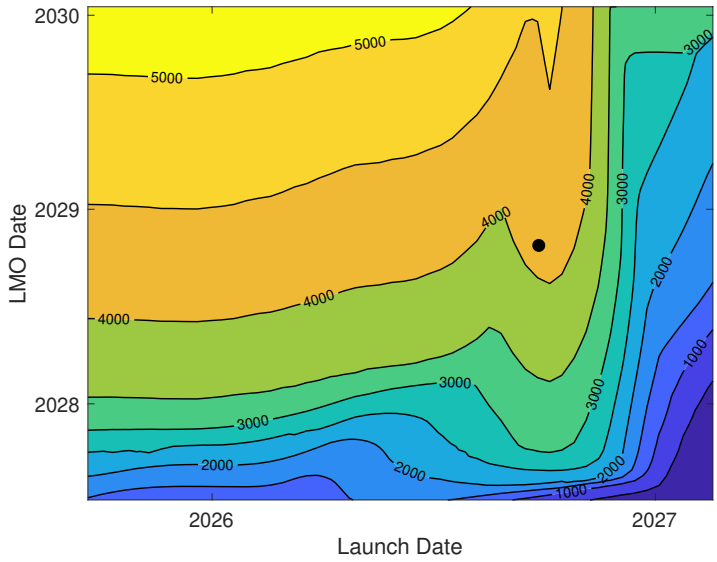

Figure 2: A bacon plot of delivered mass to low Mars orbit, in kg, over Earth launch date and LMO arrival date. The black dot is the solution selected for the baseline architecture.

launches about two months earlier. These two families are separated by a region of poor performance. Representative solutions for each family are shown side-by-side in Table 4. The early launch family launches to a lower C3 and higher initial mass compared to the late launch family. It takes a longer time to transfer to Mars, arrives at a lower velocity, and performs a larger MOI, capturing into a lower orbit around Mars. This lower capture orbit requires less time and propellant to transfer down to LMO. While both families provide similar delivered mass to LMO, the late family has the advantages of lower overall propellant mass and shorter time-of-flight. In addition, a later launch is desirable as it allows for extra development time.

Table 4: Comparison of early and late launch Earth-to-Mars solution families.

Parameter	Early Launch	Late Launch
Launch	Jun-Jul 2026	Sep-Oct 2026
LMO Arrival	Oct 2028	Oct 2028
Launch C3, km^2/s^2	3.09	5.37
Arrival v_∞, km/s	1.0	2.0
Launch Mass, kg	6400	6025
Helio. SEP Propellant, kg	529	312
Chemical Propellant, kg	1680	1328
Spiral SEP Propellant, kg	113	263
Total Propellant, kg	2322	1903
LMO Mass, kg	4078	4122
Helio. TOF, d	620	360
Spiral TOF, d	210	400

Inbound Results

Results for the inbound trajectories are shown in Figure 3 for the case of three RIT 2X thrusters at 28 kW. All solutions in the plot deliver 3000 kg of total mass to Earth at an arrival v_∞ of no greater than 4.5 km/s.

The solutions are colored by their mass at Mars departure, with lower masses indicated by the dark purple color being more desirable. For the inbound analysis, no trans-Earth injection maneuver was considered, so all trajectories depart Mars with $v_\infty = 0$. The lack of a TEI means there is less flexibility available on the return leg of the mission, resulting in large regions of infeasible departure-arrival date pairs. We can see two regions in Figure 2 that offer better performance and which are strongly tied to Earth arrival date. The first region is for arrivals in the second half of 2031, with departure dates available up through mid to late 2030. The second region covers Earth arrivals in the second half of 2033, with departures from Mars available up through late 2032.

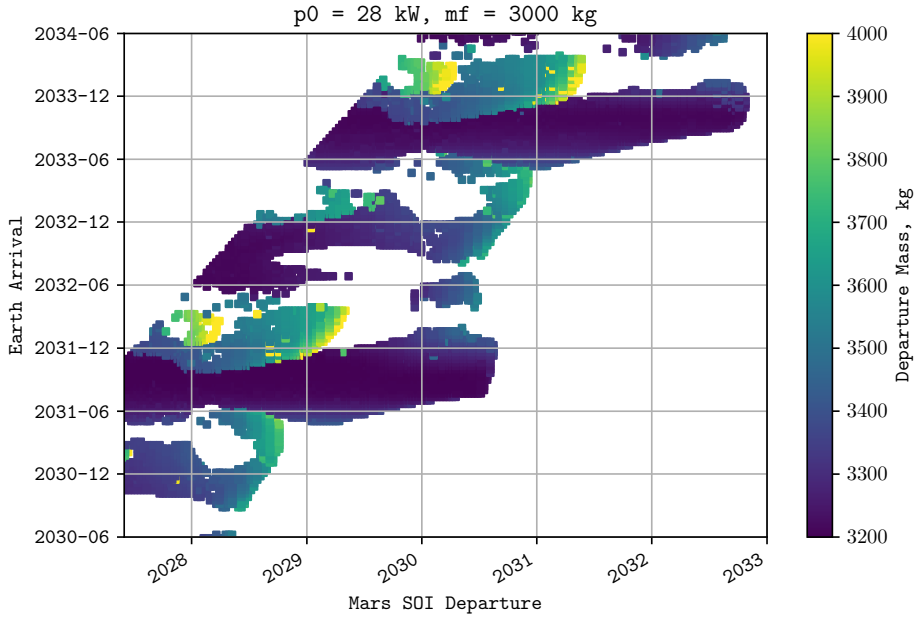

Figure 3: A scatter plot showing initial mass over Mars sphere of influence departure and Earth arrival dates.

The 2031 return opportunity is used as an example inbound trajectory. The selected trajectory departs from Mars' sphere of influence on September 8, 2030 with a mass of 3200 kg and reaches Earth on October 6, 2031. Upon Earth arrival, the spacecraft has a mass of 2940 kg and a v_∞ of 4.5 km/s. The trajectory is matched with the outbound trajectory, with a staging event while in LMO accounting for the majority of the mass difference between the outbound LMO arrival mass and the inbound LMO departure mass.

CONCLUSION

Hybrid chemical-SEP trajectories have been found to be useful for a Mars sample return mission. We have performed an extensive search of the hybrid trajectory design space for outbound trajectories to Mars and inbound trajectories back to Earth, resulting in a trajectory database that can be queried by a system optimization tool. The database covers four different thruster types, with dates spanning a 10-year time period. Power levels from 11 kW up to 120 kW were examined, along with Earth arrival masses from 750 kg to 3500 kg.

Using this database, we were able to select trajectories for baseline primary and backup opportunities which are matched with a spacecraft in an optimal architecture. A primary opportunity launching in 2026 and returning the sample to Earth in 2031 was identified using three RIT 2X thrusters at 28 kW.

ACKNOWLEDGEMENT

This research was carried out at the Jet Propulsion Laboratory, California Institute of Technology, under a contract with the National Aeronautics and Space Administration. The information provided about the Mars sample return mission concept is pre-decisional, and is provided for planning and discussion purposes only.

REFERENCES

[1] Committee on the Planetary Science Decadal Survey, "Vision and Voyages for Planetary Science in the Decade 2013-2022," tech. rep., National Research Council, 2013.

[2] N. Strange, R. G. Merrill, D. Landau, B. Drake, J. Brophy, and R. Hofer, "Human Missions to Phobos and Deimos Using Combined Chemical and Solar Electric Propulsion," *47th AIAA/ASME/SAE/ASEE Joint Propulsion Conference*, No. AIAA 2011-5663, San Diego, CA, July–August 2011.

[3] A. K. Nicholas, R. C. Woolley, A. Didion, F. Laipert, Z. Olikara, R. Webb, and R. Lock, "Simultaneous Optimization of Spacecraft and Trajectory Design for Interplanetary Missions Utilizing Solar Electric Propulsion," *29th AAS/AIAA Space Flight Mechanics Meeting*, No. AAS 19-456, Ka'anapali, HI, January 2019.

[4] J. A. Sims, P. A. Finlayson, E. A. Rinderle, M. A. Vavrina, and T. D. Kowalkowski, "Implementation of a Low-Thrust Trajectory Optimization Algorithm for Preliminary Design," *AIAA/AAS Astrodynamics Specialist Conference and Exhibit*, Keyston, CO, August 2006.

[5] Z. P. Olikara, "Framework for Optimizing Many-Revolution Low-Thrust Transfers," *AAS/AIAA Astrodynamics Specialist Conference*, No. AAS 18-332, Snowbird, UT, August 2018.

[6] R. C. Woolley and A. K. Nicholas, "SEP Mission Design Space for Mars Orbiters," *AAS/AIAA Astrodynamics Specialist Conference*, No. AAS 15-632, Vail, CO, August 2015.

[7] A. K. Nicholas, A. Didion, F. Laipert, Z. Olikara, R. C. Woolley, and R. Lock, "Mission Analysis for a Potential Mars Sample Return Campaign in the 2020's," *29th AAS/AIAA Space Flight Mechanics Meeting*, No. AAS 19-458, Ka'anapali, HI, January 2019.